Ceramic and single-crystal (1 − x)PMN–xPT constitutive behavior under combined stress and electric field loading

Kyle G. Webber [a], Ruzhong Zuo [b], Christopher S. Lynch [c],*

[a] *The George W. Woodruff School of Mechanical Engineering, The Georgia Institute of Technology, Atlanta, GA 30332, USA*
[b] *Institute of Materials Science, Darmstadt University of Technology, 64287 Darmstadt, Germany*
[c] *Department of Mechanical and Aerospace Engineering, The University of California Los Angeles, 36-146 Engineering IV, 420 Westwood Plaza, Los Angeles, CA 90095-1597, USA*

Abstract

Pb(Mg$_{1/3}$Nb$_{2/3}$)O$_3$–0.32(PbTiO$_3$), PMN–0.32PT, single crystals have been characterized under combined stress and electric field loading [McLaughlin EA, Liu T, Lynch CS. Relaxor ferroelectric PMN–32%PT crystals under stress and electric field loading: I-32 mode measurements. Acta Mater 2004;52:3849, McLaughlin EA, Liu T, Lynch CS. Relaxor ferroelectric PMN–32%PT crystals under stress, electric field and temperature loading: II-33-mode measurements. Acta Mater 2005;53:4001] [1–3]. This approach is extended to PMN–0.26PT single crystals to explore the effect of composition on field driven phase transformations and to PMN–0.32PT ceramic specimens to compare with polycrystalline behavior. Electric displacement and strain were measured as a function of combinations of stress and both unipolar and bipolar electric fields. The single-crystal results indicate that compositions further from the morphotropic phase boundary require higher driving forces for field induced phase transformations. Evidence of these transformations is not apparent in the results from the ceramic specimens.
© 2007 Acta Materialia Inc. Published by Elsevier Ltd. All rights reserved.

Keywords: Relaxor; Phase transformation; Ferroelectric; Constitutive behavior; Single-crystal

1. Background

Over the past 15 years, considerable effort has been devoted to characterizing the response of ferroelectric ceramics to combined stress and electric field loading [3–6]. This work has led to the development of micromechanical constitutive laws that predict the macroscale material behavior based on a volume average of the behavior at the microscale [7–9]. At the microscale, the material behavior has been modeled using a simplified hysteresis behavior due to a lack of single-crystal data. The recent advancements in crystal growth techniques have led to the availability of large size single-crystal relaxor ferroelectrics for characterization. This has made clear that single-crystal hysteresis behavior is far more complex than initially assumed and not only includes effects of domain wall motion, but also the effects of multiple field induced phase transformations.

Previous work characterizing the response of PMN–0.32PT single crystals to combined stress and electric field loading has led to the question of whether this measured single-crystal behavior can be used to predict the behavior of polycrystalline ceramics of the same composition through micromechanical modeling. Such models would take into account effects of orientation, intergranular interactions, ferroelectric and ferroelastic polarization reorientation and field induced phase transformations, and use volume averaging techniques to predict the material behavior at the macroscale. These models would be extremely useful in providing a fundamental understanding of the behavior of ceramics, including textured ceramics and thin

---

* Corresponding author. Tel.: +1 310 825 7660.
   E-mail address: cslynch@seas.ucla.edu (C.S. Lynch).

films, under large in-plane biaxial stress. To date there have not been sufficient experimental data on single-crystal and ceramic specimens of the same composition to construct micromechanical models without the introduction of gross simplifications. It is hoped that this work will provide data that will contribute to the development of more accurate micromechanical models. It begins with a review of the measured behavior of single-crystal and ceramic ferroelectric materials. This is followed by the presentation of the results of characterizing the response of single-crystal PMN–0.26PT and ceramic PMN–0.32PT and discussion thereof.

The response of relaxor single crystals to combined stress and electric field loading has been discussed by various authors. McLaughlin et al. characterized the response of PMN–0.32PT single crystals oriented in the [001] and [011] directions at various temperatures [1,2]. In this work, the electric displacement and strain were measured as a function of stress, electric field and temperature. The results were presented as three-dimensional surface plots showing the effects of field induced phase transformations. Phase transformation maps were created which showed the dependence of these transformations on applied electric field, stress and temperature. Park and Shrout [10] measured the d_{33} piezoelectric coefficient as a function of composition for the [001] and [111] oriented $Pb(Zn_{1/3}Nb_{2/3})O_3–0.045(PbTiO_3)$, PZN–0.045PT, single crystals. In addition, the electric displacement and strain were measured in response to bipolar and unipolar electric field loading, respectively, for crystal cuts between the [001] and [111] orientations. Liu and Lynch [11,12] have measured the unipolar and bipolar response of PZN–0.045PT for a series of crystal cuts. A cyclic electric field was applied at multiple angles between the [001] and [111] orientation directions. The results showed that the effects of domain wall motion on the hysteresis behavior are strongly orientation dependent. Liu and Lynch characterized the electromechanical response of PZN–0.045PT single crystals for the [001], [011] and [111] orientations [13]. This work utilized a combination of measured piezoelectric coefficients together with orthogonal transformations to determine a full set of piezoelectric coefficients in the single domain [111] orientation. This study also presented measured double loop behavior, evidence of an electric field induced phase transformation. The hysteretic phase transformation was shown to be accompanied by a jump in strain and electric displacement in contrast to the more gradual electric field induced phase transformation seen in PMN–xPT specimens [14].

Recent X-ray diffraction studies have shown that PMN–xPT single crystals at room temperature and at zero stress and zero electric field are in a rhombohedral phase when $x < 0.3$ and a tetragonal phase when $x > 0.35–0.37$ [15,16]. Studies have also shown that PMN–xPT and PZN–xPT specimens near the morphotropic phase boundary (MPB) have an intricate multiphase state consisting of tetragonal, rhombohedral, orthorhombic and monoclinic

phases [16–18]. The phase of PMN–xPT and PZN–xPT is dependent on applied fields such as stress, electric field and temperature, in addition to the composition. Many researchers have shown experimental evidence of rhombohedral to orthorhombic (R–O) [1,2,14,19,20] and rhombohedral to tetragonal (R–T) [10,21,22] phase transformations in relaxor single crystals under external fields. Viehland and Li [20] measured the unipolar and bipolar strain and electric displacement during electric field induced R–O phase transformation in ⟨110⟩ oriented PMN–0.3PT single-crystal specimens. McLaughlin et al. showed evidence that electric field [1] and stress [2] are both capable of inducing a R–O phase transformation in PMN–0.32PT single crystals with an engineered domain state. Zhao et al. [19] confirmed an R–T phase transition in PMN–0.31PT single crystals with powder X-ray diffraction. Ren et al. [22] measured the ⟨001⟩ electric field induced R–T phase transformations of PZN–0.045PT and PZN–0.8PT single crystals at varying temperatures. This work showed that the electric field required to initiate an R–T phase transition decreased linearly with an increase in temperature.

Many researchers have worked on the characterization of major hysteresis loops in ferroelectric ceramics under combined stress and electric field loading [3–6]. Cao and Evans [4] investigated electromechanical coupling and irreversibility in ferroelectric ceramics. In their study, hard and soft PZT specimens, a relaxor material (PMN–0.1PT) and an antiferroelectric (PLSn$_{0.27}$ZT) were poled and subjected to a uniaxial compressive stress. Several significant observations were made. First, when a compressive stress was applied normal to the polarization direction, 180° switching was inhibited (increased coercive field). Second, nonlinear deformation was related to the deviatoric components of stress and strain. Third, when uniaxial stress was applied to a specimen parallel to the polarization there was a subsequent change in the Poisson ratio as the load was increased that was associated with a transition from ferroelastic switching to purely elastic strain. They also proposed a material-specific constitutive law. Lynch [3] characterized the large field electromechanical behavior of lanthanum doped 8/65/35 PLZT. In this study, initially unpoled PLZT specimens were subjected to a uniaxial stress and electric field. This work provided measurements of the strain/electric field, polarization/electric field, stress/polarization and stress/strain hysteresis loops. It also provided several observations along with a discussion of the possibility of modeling the intergranular stress effects using a variation of an Eshelby inclusion model [23] for intergranular constraints. More recent experimental efforts have focused on characterizing ferroelectric materials under other loading. Huber and Fleck [5] and Zhou et al. [6] have looked at the multiaxial electrical switching of ferroelectric ceramics and Chen and Lynch [24] characterized 8/65/35 PLZT tubes under multiaxial mechanical loading.

This study presents a comparison of the measured large field constitutive behavior of ceramic PMN–0.32PT and

single-crystal PMN–0.26PT. It also presents a comparison of measured single-crystal behavior with previously published results for single-crystal PMN–0.32PT. This gives a direct indication of the effect of composition (proximity to the MPB) on the single-crystal behavior. The results are discussed in terms of the effects of domain wall and phase boundary motion.

2. Experimental methodology

This section describes the specimen preparation, the experimental arrangement and the results of the single-crystal and ceramic characterization.

2.1. Specimen preparation

2.1.1. Single-crystal specimen manufacturing and preparation

PMN–0.26PT and PMN–0.32PT are each in the rhombohedral phase at room temperature, with the PMN–0.32PT being very close to an MPB. The spontaneous polarization of the rhombohedral phase lies in one of the eight possible $\langle 111 \rangle$ directions. When an electric field in excess of the coercive field is applied in the [001] direction as shown in Fig. 1, the spontaneous polarization will reorient such that four of the eight possible $\langle 111 \rangle$ crystal variants are present.

The single-crystal specimens were provided by TRS Technology Inc. Specimens are cut from a single-crystal boule. Each specimen measured $5 \times 5 \times 5$ mm and was oriented with the [001] (cubic referenced) crystallographic axis parallel with the mechanical and electrical loading direction. No further polishing or cutting was preformed on the specimens. Prior to testing, each crystal was cleaned in an ultrasonic cleaner with acetone followed by ethanol. Two opposing faces were sputtered with a thin layer of gold to serve as electrodes. Three cubes were stacked and bonded together and the center cube was instrumented with strain gages. Testing was done in this manner to increase the aspect ratio and to produce a uniform uniaxial stress in the center specimen (where strain was measured) by decreasing clamping effects at the edges during loading. Buehler Crystal bond mounting wax was used to bond the electroded sides of each specimen together to maintain
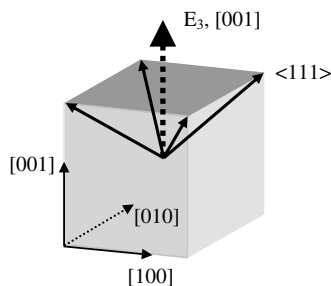
alignment of each crystal relative to one another. A copper foil mesh with a thickness of 0.025 mm was placed between each crystal in the bonded region for electrical contact. A schematic of this experimental setup is shown in Fig. 2.

2.1.2. Ceramic specimen manufacturing and preparation

The PMN–0.32PT ceramic was manufactured at the Darmstadt University of Technology, Darmstadt, Germany. The chemicals used to produce these specimens were PbO (>99.0%; Alfa Aesar, Germany), $MgCO_3Mg(OH)_2 \cdot 6H_2O$ (99.5%; Alfa Aesar, Germany), Nb_2O_5 (99.9%; ChemPur, Germany) and TiO_2 (99.9%; Alfa Aesar, Germany). The columbite precursor method was employed to prepare $68Pb(Mg_{1/2}Nb_{2/3})O_3–32PbTiO_3$ powder. The columbite, $MgNb_2O_6$ (MN), was synthesized by attrition-milling $MgCO_3Mg(OH)_2 \cdot 6H_2O$ and Nb_2O_5 for 12 h, followed by calcination at 1200 °C for 4 h. The dried MN powder, PbO and TiO_2 were weighed according to the stoichiometric formula and ball-milled in ethanol for 24 h with a planetary mill and yttrium-stabilized zirconia balls of 5 mm in diameter. The mixed powder was then calcined in an alumina crucible at 850 °C for 2 h. After calcination, the powder was further ground for 24 h using the above-mentioned ball mill. Rectangular bars were uniaxially pressed in a stainless steel die, followed by a cold isostatic pressing at 300 MPa. Sintering was conducted in air at 1200 °C for 3 h at a heating rate of 300 °C h^{-1}, with the specimens buried in powder of the same composition to minimize the lead volatilization, and covered with double alumina crucibles as well. After that, the sintered specimens were ground and polished on all sides until the defined dimensions of $8 \times 8 \times 12$ mm were reached.

Prior to testing, each specimen was cleaned in an ultrasonic cleaner with acetone followed by ethanol. Gold electrodes were sputtered onto opposing 8×8 mm faces.

2.2. Experimental arrangement

Mechanical and electrical loads were applied simultaneously using the fixture shown in Fig. 3. Uniaxial compressive load was applied by a screw-type load frame. The bottom of the specimen rested on a steel plate which was attached in series with a capacitor to ground potential.

Fig. 1. Possible variants in the [001] poled rhombohedral phase.
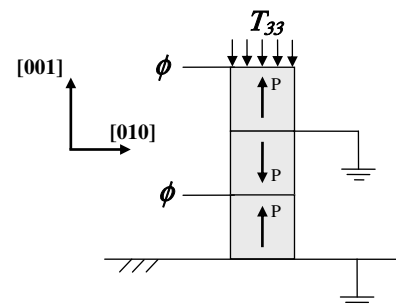

Fig. 2. Three single-crystal specimens were bonded and subjected to electrical and mechanical loading as shown.
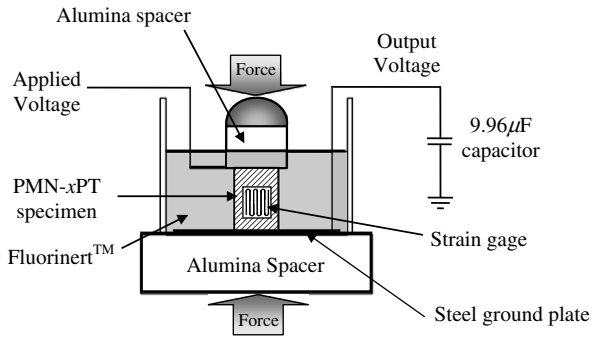
Fig. 3. Schematic of testing arrangement.

During testing, each specimen was submerged in a bath of Fluorinert™ FC-70 electrical liquid. Electrical isolation from the load frame was accomplished by placing alumina blocks above and below each specimen.

2.3. Data measurement methodology

The analog output signal of each instrument was recorded using an analog-to-digital data acquisition system.

2.3.1. Strain

Strain gages were attached to all specimens. Strain for the ceramic specimens was measured both longitudinal (X_3) and transverse (X_1, X_2) to the direction of the polarization. Two longitudinal/transverse 90° strain gage rosettes were attached to opposing faces of the ceramic, while on the other two faces strain gages measuring only the longitudinal strain were attached. Fig. 4a illustrates the strain gage orientation used on each ceramic specimen. Due to their smaller size, single-crystal specimens were only instrumented with two longitudinal strain gages on opposing faces. Fig. 4b shows the strain gage placement on the single-crystal specimens. The Micro-Measurements 2110A strain gage signal conditioner output was recorded. The strain measurements were averaged to obtain an average material response.

2.3.2. Electric field

A triangular wave at 0.02 Hz was applied to the top electrode, with the bottom electrode connected to ground. A Wavetek DDS Model 29 function generator was used to create the reference signal that was amplified 2000 times using a TREK Model 20/20A amplifier. The monitor voltage from the amplifier was recorded.

2.3.3. Load

Load was applied using a DDL screw-type load frame with a 4.45 kN load cell. Rubber blocks were placed under the testing fixture in the load path to create sufficient compliance to maintain a constant load condition during electrical excitation of the piezoelectric material.

2.3.4. Electric displacement

The electric displacement was measured by monitoring the voltage across a 9.96 μF capacitor in a Sawyer–Tower arrangement. The capacitor was connected from the bottom electrode of the specimen to ground. The voltage across the capacitor was measured using a high input impedance Keithley 6512 electrometer. The analog output signal of the electrometer was recorded.

3. Experimental results

Experimental measurements of longitudinal strain and electric displacement are presented for single-crystal and ceramic PMN–xPT specimens. The resolutions of each measurement or load application system are listed here: the strain measurement system is capable of resolving ±50 microstrain, the electric displacement measurements have a resolution of ±0.01 C m^{-2}, the load cell has an accuracy of ±13 N and the electric field application system has an accuracy of ±0.01 kV mm^{-1}. In most of the measurements the precision was on the order of 10% of the accuracy. The noted exception is in some of the electric displacement measurements, where a spurious electrical signal resulted in noise superimposed on the desired signal. In cases other than these, error bars would be smaller than the data markers and thus have not been included. In the
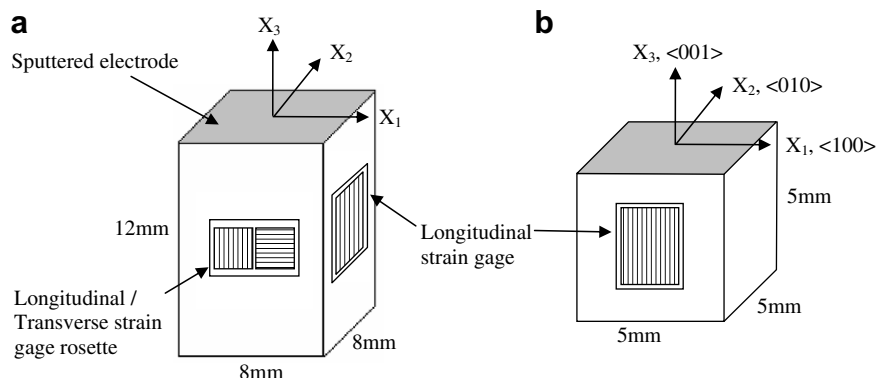

Fig. 4. Specimen showing the strain gage configuration for (a) the ceramic specimens and (b) the single-crystal specimens.

cases where electrical noise contributed to the error, data markers are included in the chart.

3.1. Bipolar PMN–0.26PT single-crystal

Fig. 5 shows the two-dimensional plots of the longitudinal strain (Fig. 5a) and electric displacement (Fig. 5b) under room temperature (20 °C) bipolar electric field loading at various constant stress levels (–0.4, –16, –32, –48, –64 MPa). The dotted line in Fig. 5a was added to illustrate the reduction in coercive field associated with applied stress.

3.2. Unipolar PMN–0.26PT single-crystal experimental results

Fig. 6a shows the electric displacement plotted against the applied unipolar electric field. Fig. 6b shows the longitudinal strain response to applied electric field at constant compressive stress levels. Fig. 6c displays the electric displacement change during compressive stress loading at constant electric field bias levels. Fig. 6d illustrates the longitudinal strain during application of unipolar stress at constant electric field levels.
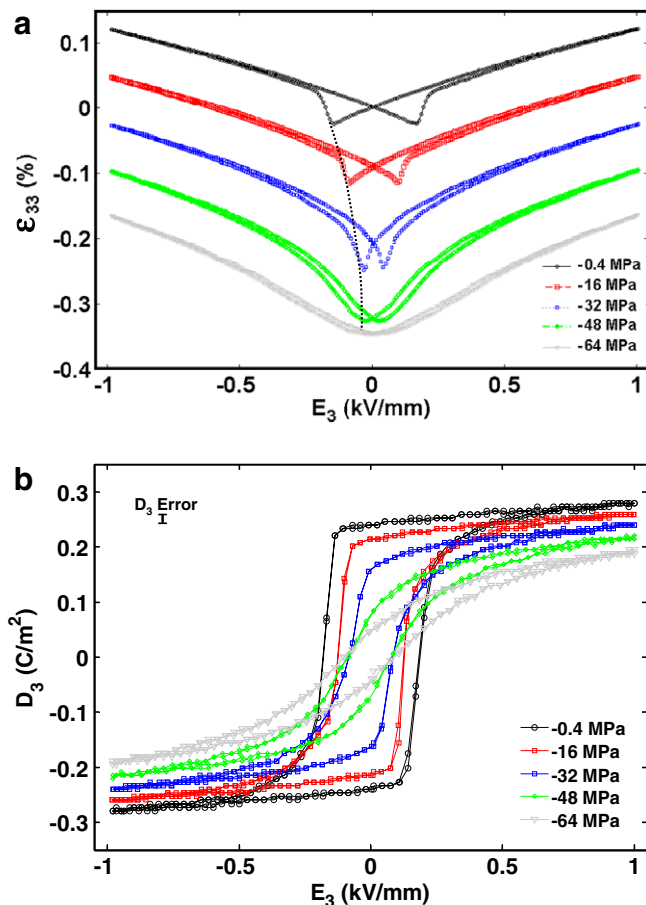
The interactions of the nonlinearities can be visualized using a three-dimensional plot. Fig. 7 shows the three-dimensional plots produced from the unipolar loading data.

3.3. Stress-induced polarization reversal

Fig. 8 shows the measured electric displacement during mechanical loading with a bias field of 0.008 kV mm^{-1} (a small fraction of the coercive field) applied to the specimen. The solid line represents the electric displacement when the electric field and polarization direction are initially in the same direction. The dotted line shows the electric displacement curve when the electric field is applied opposite to the initial polarization direction.

3.4. PMN–0.32PT ceramic

In the ceramic specimens, the strain response varied between the four gages during the stress induced polarization reorientation. It was determined that this was not an alignment issue or a problem with the loading fixture. Specimens were removed, rotated and replaced and the loading repeated multiple times. Each time, the same side always gave the same behavior. These specimens subjected to compressive stress depolarization did not ferroelastically dipole uniformly. The ferroelastic behavior consistently started at one side and moved across the specimen. The results presented are the averages obtained from the four strain gages.

Fig. 9 displays the experimental results for the mechanical and electrical loading of ceramic specimens of PMN–0.32PT. Multiple specimens were tested and the results shown here are representative of all the specimens tested.

4. Discussion

The nonlinearity observed in the PMN–0.26PT single crystals (Figs. 5–7) is indicative of a phase transformation driven by the applied compressive stress in the [0 0 1] direction. A schematic of the crystal variants believed to be present in the two phases is shown in Fig. 10. Before load was applied to the single-crystal it was in the rhombohedral phase near the MPB. There are eight possible variants in the rhombohedral phase. This is reduced to four when a single-crystal material in the rhombohedral phase is poled in the [0 0 1] orientation. In the unstressed four-variant state, the polarized crystal displayed a linear response to the applied electric field. As mechanical stress was increased, a phase transition from rhombohedral with ⟨1 1 1⟩ spontaneous polarization to what is most likely orthorhombic with spontaneous polarization in the ⟨0 1 1⟩ orientation took place. Due to the limited hysteresis and the continuous nonlinear change in elastic, dielectric and piezoelectric crystal properties observed during the phase transformation, it appears that there was either a continuous rotation of the polarization through an intermediate monoclinic phase or a continuous evolution of the volume fraction of the orthorhombic phase as applied stress was

Fig. 5. (a) Longitudinal strain and (b) electric displacement measured during combined mechanical and electrical loading.
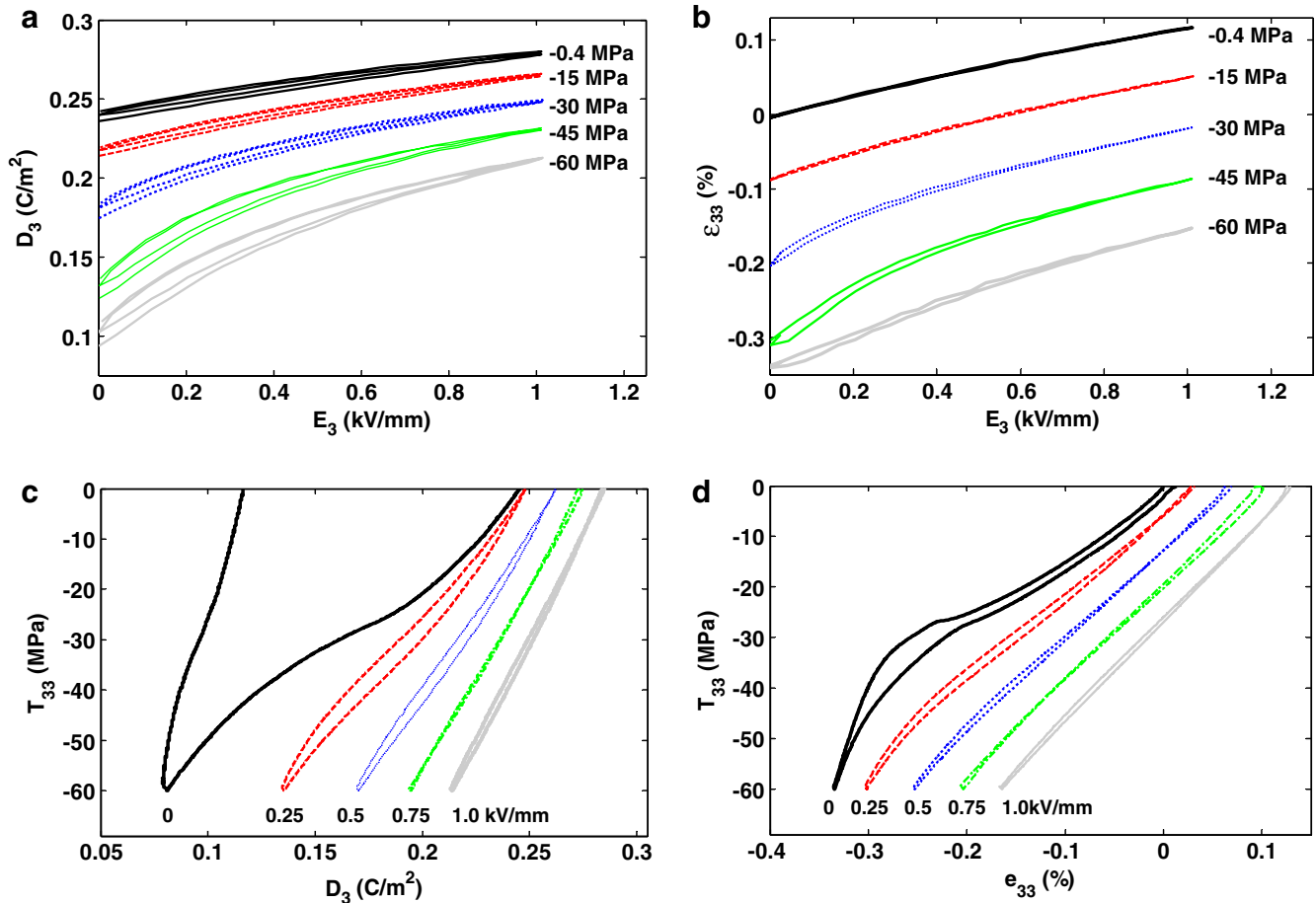
Fig. 6. Two-dimensional plots of mechanical and electrical unipolar loading at 20 °C. (a) Electric displacement vs. applied electric field at constant stress levels, D_3–E_3; (b) longitudinal strain vs. electric field at constant stress levels, ε_{33}–E_3; (c) electric displacement vs. stress at constant electric field bias levels, D_3–σ_{33}; and (d) longitudinal strain vs. stress at constant electric field bias levels, ε_{33}–σ_{33}.

increased. Upon unloading of the mechanical stress, the crystal structure transformed back into the rhombohedral phase with a small amount of hysteresis.

Mechanical load in the [0 0 1] crystallographic orientation depolarizes the single-crystal by switching it to a perpendicularly polarized phase. A single-crystal with [0 0 1] orientation in the orthorhombic phase which has four possible variants perpendicular to the applied mechanical load is fully depolarized and has an effective d_{333} piezoelectric coefficient of zero. This behavior is seen the Figs. 5a and 6b. The degeneration of the hysteresis loops from butterfly shape to quadratic electrostriction can be explained in terms of an orthorhombic phase with field induced rotation through a monoclinic phase. At high compressive stress the material is fully depolarized with the orthorhombic crystal variants lying perpendicular to the stress direction. As the electric field is increased the spontaneous polarization begins to rotate through the monoclinic phases towards the rhombohedral phase. This results in the observed quadratic electrostrictive behavior seen in the bottom curve of Fig. 5b.

The coercive field is the magnitude of the reverse electric field required to reorient the remnant polarization of a ferroelectric material and has been identified in Figs. 5a and 9a as the location where the butterfly loops are at the lowest

value. When an electric field that opposes the polarization has been increased to the point where local resistance to polarization switching is overcome, the dipoles reorient and the longitudinal strain begins to increase. Application of a mechanical load decreases the coercive field (reduces the energy barrier to polarization reversal) by driving the material toward a phase that has zero barrier to polarization reorientation (the perpendicular orthorhombic variants). The reduction of coercive field values due to mechanical loading is shown by the dotted line in Figs. 5a and 9a. Both the ceramic and single-crystal specimens show a decreasing coercive field, although the effect in the single-crystal is far more pronounced. The ceramic specimens initially had a larger coercive field than that of the single-crystal specimens. This may be due to a number of factors including grain size effects, orientation effects, intergranular interactions and the effects of inhomogeneities such as porosity and inclusions. These inhomogeneities create local fields that can affect macroscopic constitutive behavior by either inhibiting or generating domain wall motion and phase transformations within single-crystal grains.

Comparison of Figs. 5 and 9 show that during bipolar loading there was more hysteresis in the ceramic than the single-crystal. The single-crystal is in a domain engineered
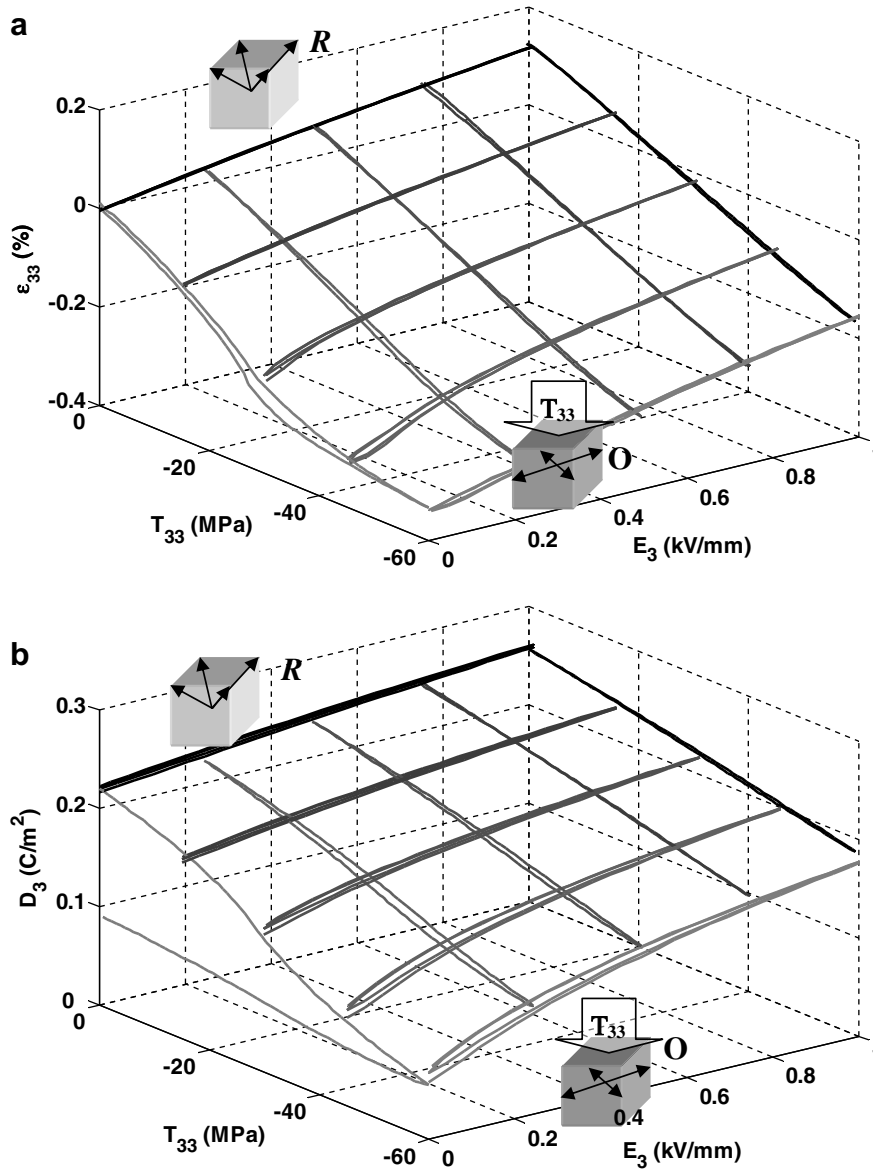
Fig. 7. Three-dimensional phase transformation map of (a) strain as a function of stress and electric field, ε_{33}–E_3–T_{33}; and (b) electric displacement as a function of stress and electric field, D_3–E_3–T_{33}.

state in which the driving forces for non-180° domain wall motion are minimal. This results in the single crystals having a high degree of linearity and very low hysteresis in their unipolar response. When the crystals are cut at different angles this changes significantly. Measurements on PZN–0.045PT single crystals cut at various angles [11,12] have shown that when the electric field direction is rotated from [0 0 1] toward [1 1 1] the strain–electric field hysteresis loops open up and change shape. If the behavior in the PMN–0.26PT is analogous, the orientation effect may play a significant role in causing the differences between the single-crystal and ceramic specimens. The orientation distribution of the grains in the ceramic will ensure that there will always be grains oriented such that there will be a driving force for non-180° domain wall motion. This domain wall motion will interact with the grain boundaries resulting in intergranular local stress and electric fields. These

fields can contribute to hysteresis. Grain boundary or bulk charge migration within the ceramic can interact with domains and can also contribute to hysteresis.

At very low stress it can be seen in Fig. 5a and b that the single-crystal specimen had a linear strain and electric displacement response to the applied electric field. It can be seen in Fig. 9a and b that during preload the initial response of the ceramic to an applied electric field was nonlinear.

Evidence of a phase transformation can be seen in the three-dimensional plots (Fig. 7). The [0 0 1] oriented single-crystal can be driven to a different phase through the application of a compressive stress in the [0 0 1] direction and can be subsequently pulled back from that phase to the rhombohedral phase through an electric field in the [0 0 1] direction. This illustrates that the applied stress and electric field act as competing driving forces. The dotted
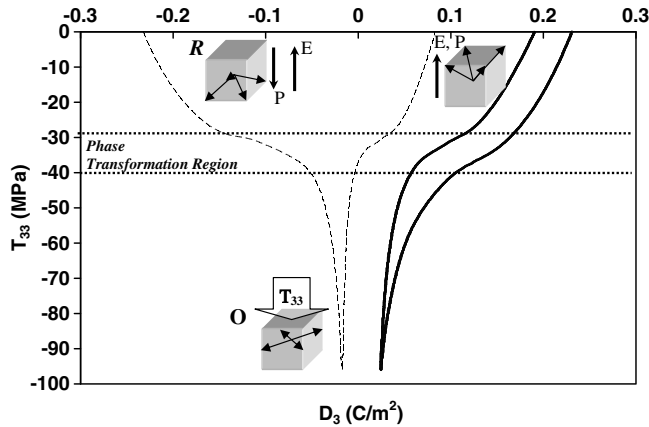
Fig. 8. The stress induced depolarization in the presence of a small bias electric field of 0.008 kV mm^{-1} shows the effect of the stress reducing the coercive field to near zero.
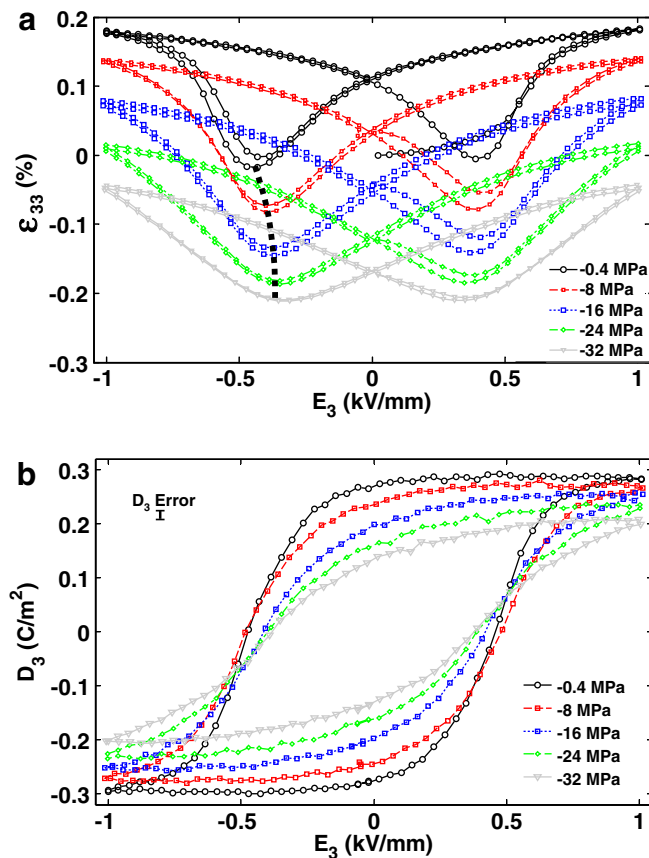

Fig. 9. (a) Longitudinal strain and (b) electric displacement vs. electric field at various preload stress levels.
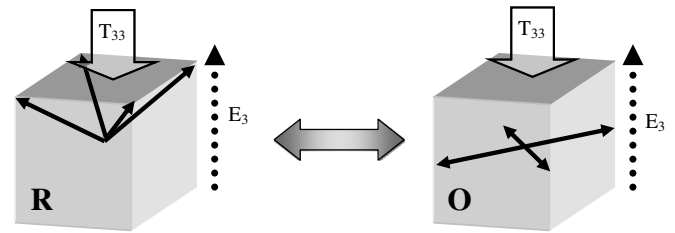

Fig. 10. Phase transformations between the rhombohedral and orthorhombic phases induced by stress [1].

is closer to the MPB than PMN–0.26PT [16]. The PMN–0.32PT and PMN–0.26PT show similar material behavior; however, there are important differences that show the compositional dependence of constitutive behavior. The piezoelectric coefficient of PMN–0.32PT was reported as 2100 pC N^{-1}, which is ∼42% larger than that measured in the PMN–0.26PT material. In addition, it is also apparent that lowering the amount of PT increases the stress at which a phase transformation initiates, while simultaneously increasing the material stiffness. PMN–0.26PT shows the beginning of a phase transition region when no electric field was applied at ∼–34 MPa, while in PMN–0.32PT the phase transformation began at ∼–20 MPa. The trend is that as the composition is moved away from the MPB, on the rhombohedral side, the stiffness increases, the piezoelectric coefficients decrease, the dielectric constant decreases and the energy barrier to the phase transformation increases.

Fig. 8 shows the stress induced depolarization of the single-crystal material in the presence of an electric field well below the coercive field. During a unipolar stress cycle in the absence of an applied electric field it was shown that single-crystal PMN–0.26PT was driven to the depolarized orthorhombic phase. Without a suitable externally applied driving force, such as a small bias electric field, the spontaneous polarization direction can reorient in either the [1 1 1] or [1 1 1̄]. This results in the strain returning to the original preload value when the stress is unloaded, while the electric displacement does not recover. However, when the mechanical loading/unloading cycle is performed in the presence of a small electric field, a very small driving force is provided that induces a preferred orientation in the dipoles when the stress is removed.

From ceramic behavior shown in Fig. 9 it can be seen that the amount of hysteresis present during bipolar electric field loading decreased as the uniaxial stress was increased. This may be due to the local barriers to switching being overcome by the applied mechanical energy. The ceramic specimens initially had a nonlinear response to the electric field. When the electric field reached a critical level the response became approximately linear. This is in contrast to the behavior of the single-crystal, where the initial behavior was linear and nonlinearity was induced by applied stress.

A summary of the measured elastic, piezoelectric and dielectric coefficients of the single-crystal and ceramic specimens is presented in Table 1. These values were obtained

line in Fig. 7 approximately represents the dividing line between the rhombohedral phase and the phase transition region. This same general behavior was seen in earlier experimental characterization of PMN–0.32PT single crystals [2]. In that study, [0 0 1] oriented single-crystal specimens were subjected to combined unipolar electromechanical loading at various temperatures, with the resulting strain and electric displacement measured. PMN–0.32PT

Table 1
Elastic, piezoelectric and dielectric material properties for single-crystal PMN–0.26PT and ceramic PMN–0.32PT

Material property	Single-crystal PMN–0.26PT		Ceramic PMN–0.32PT
	R	O	
Compliance, $S_{3333}^E (10^{-12} \text{ m}^2/\text{N})$	59.5	12.4	13.5
Piezoelectric, d_{333} (pm/V)	1475	–	1350
$d_{311} = d_{322}$ (pm/V)	–	–	−550
Relative permittivity, $\varepsilon_{33}^T/\varepsilon_0$ ($\varepsilon_0 = 8.855 \times 10^{-12}$ F/m)	5500	–	8385

by measuring the initial slope of the corresponding strain or electric displacement vs. electric field curves.

5. Concluding remarks

The single-crystal behavior depends on various factors and nonlinear processes such as crystal orientation angle, crystal cut, temperature, phase transformation behavior and domain wall motion. The ceramic behavior is the result of a complex arrangement of these effects in addition to effects of intergranular interactions and dispersed inhomogeneities. This creates a complex network of nonlinear local effects which can influence overall material constitutive behavior.

The strain and polarization of [001] single-crystal PMN–0.26PT and ceramic PMN–0.32PT specimens were characterized in response to combined large electric field and stress. Testing was done at room temperature. Single-crystal specimens showed clear evidence of a stress induced phase transformation from the rhombohedral phase to the depolarized assumed orthorhombic phase. It was also shown that an electric field applied in an opposing direction to the stress was able to overcome the applied stress and return the specimen to the rhombohedral phase. Three-dimensional plots were created from the measured single-crystal unipolar longitudinal strain and electric displacement response to applied loads. Ceramic specimens were characterized under bipolar electric fields at various stress levels.

References

[1] McLaughlin EA, Liu T, Lynch CS. Relaxor ferroelectric PMN-32%PT crystals under stress and electric field loading: I-32 mode measurements. Acta Mater 2004;52:3849.

[2] McLaughlin EA, Liu T, Lynch CS. Relaxor ferroelectric PMN-32%PT crystals under stress, electric field and temperature loading: II-33-mode measurements. Acta Mater 2005;53:4001.

[3] Lynch CS. The effect of uniaxial stress on the electro-mechanical response of 8/65/35 PLZT. Acta Mater 1996;44:4137.

[4] Cao H, Evans AG. Nonlinear deformation of ferroelectric ceramics. J Am Ceram Soc 1993;76:890.

[5] Huber JE, Fleck NA. Multi-axial electrical switching of a ferroelectric: theory versus experiment. J Mech Phys Solid 2001;49:785.

[6] Zhou D, Kamlah M, Laskewitz B. In: William D. Armstrong, editor. Smart structures and materials 2006: active materials: behavior and mechanics, International Society for Optical Engineering, Bellingham (WA); 2006. p. 617009.

[7] Hwang SC, Lynch CS, McMeeking RM. Ferroelectric/ferroelastic interactions and a polarization switching model. Acta Metall Mater 1995;43:2073.

[8] Chen W, Lynch CS. Model for simulating polarization switching and AF-F phase changes in ferroelectric ceramics. J Intell Mater Syst Struct 1998;9:427.

[9] Fan J. A meso-electro-mechanical model for PMN-PT-BT ceramics behavior. J Intell Mater Syst Struct 2004;15:203.

[10] Park S-E, Shrout TR. Ultrahigh strain and piezoelectric behavior in relaxor based ferroelectric single crystals. J Appl Phys 1997;82:1804.

[11] Liu T, Lynch CS. Orientation dependence of nonlinearity and hysteresis in PZN-4.5%PT single crystals I: unipolar response. J Intell Mater Syst Struct 2006;17:953.

[12] Liu T, Lynch CS. Orientation dependence of nonlinearity and hysteresis in PZN-4.5%PT single crystals II: bipolar electromechanical response. J Intell Mater Syst Struct 2006;17:931.

[13] Liu T, Lynch CS. Ferroelectric properties of [110], [001] and [111] poled relaxor single crystals: measurements and modeling. Acta Mater 2003;51:407.

[14] Liu T, Lynch C. Characterization and modeling of relaxor single crystals. Integr Ferroelectr 2005;71:173.

[15] Singh AK, Pandey D. Structure and the location of the morphotropic phase boundary region in $(1 - x)[Pb(Mg_{1/3}Nb_{2/3})O_3] - xPbTiO_3$. J Phys Condens Mat 2001;13:931.

[16] Noheda B, Cox DE, Shirane G, Ye Z-G, Gao J. Phase diagram of the ferroelectric relaxor $(1 - x)PbMg_{1/3}Nb_{2/3}O_3 - xPbTiO_3$. Phys Rev B 2002;66:054104.

[17] Ye ZG. Crystal chemistry and domain structure of relaxor piezocrystals. Curr Opin Solid State Mater Sci 2002;6:35.

[18] Singh AK, Pandey D. Evidence for M_B and M_C phases in the morphotropic phase boundary region of $(1 - x)[Pb(Mg_{1/3}Nb_{2/3})O_3] - xPbTiO_3$: a Rietveld study. Phys Rev B: Condense Mater Mater Phys 2003;67:064102.

[19] Zhao X, Wang J, Luo H, Chan HLW, Choy CL. Effect of a bias field on the dielectric properties of $0.69Pb(Mg_{1/3}Nb_{2/3})O_3 - 0.31PbTiO_3$ single crystals with different orientations. J Phys Condens Mater 2003;15:6899.

[20] Viehland D, Li JF. Anhysteretic field-induced rhombhohedral to orthorhombic transformation in ⟨110⟩-oriented $0.7Pb(Mg_{1/3}Nb^{2/3})-O^3 - 0.3PbTiO^3$ crystals. J Appl Phys 2002;92:7690.

[21] Liu S-F, Park S-E, Shrout TR, Cross LE. Electric field dependence of piezoelectric properties for rhombohedral $0.955Pb(Zn_{1/3} Nb_{2/3})O_3 - 0.045PbTiO_3$ single crystals. J Appl Phys 1999;85:2810.

[22] Ren W, Liu SF, Mukherjee BK. Piezoelectric properties and phase transitions of ⟨001⟩-oriented $Pb(Zn_{1/3}Nb_{2/3})O_3$–$PbTiO_3$ single crystals. Appl Phys Lett 2002;80:3174.

[23] Eshelby JD. The elastic field outside an ellipsoidal inclusion. Proc Royal Soc London, Ser A 1959;252:561.

[24] Chen W, Lynch CS. Multiaxial constitutive behavior of ferroelectric materials. J Eng Mater Technol, Trans ASME 2001;123:169.